APPLICATIONS OF
MODELLING AND SIMULATION
http://arqiipubl.com/ams eISSN 2600-8084 VOL 8, 2024, 191-200

Multi-Mode Input Shapers for Oscillation Control of an Overhead Crane with Distributed Mass Payload

M. M. Bello[1,2], Z. Mohamed[1*], S. M. Fasih ur Rehman[3], W. A. Balogun[1], K. Aibek[4] and S. Gamzat[5]

[1]Faculty of Electrical Engineering, Universiti Teknologi Malaysia, 81310 UTM Johor Bahru, Johor, Malaysia
[2]Department of Mechatronics Enginering, Faculty of Engineering, Bayero University, 3011 Kano, Nigeria
[3]Department of Electronics Enginering, Faculty of Engineering, The Islamia University of Bahawalpur, Punjab, Pakistan
[4]Automation and Control Department, Faculty of Technology, Taraz Regional University, Taraz, Kazakhstan
[5]Department of Automation and Manufacturing Processes, Abylkas Saginov Karaganda Technical University, Karaganda, Kazakhstan

[*]Corresponding author: zahar@fke.utm.my

Submitted 01 April 2024, Revised 03 June 2024, Accepted 21 June 2024, Available online 27 June 2024.

Abstract: A crane system with distributed mass payload (DMP) is highly nonlinear and it is a multi-mode system with different oscillation frequencies. The crane dynamics are also largely affected when operating under different cable and payload lengths. This paper investigates robust multi-mode input shapers for effective oscillation control of an overhead crane carrying DMP. Three robust shapers which are Zero Vibration Derivative (ZVD), Extra-Insensitive (EI) and Equal Shaping-Time and Magnitude (ETM) are considered and modified to be multi-mode shapers. These are obtained by convolving two input shapers that are designed separately based on the hook and payload oscillation frequencies. To assess the effectiveness of the shapers, Matlab simulations are performed by using the nonlinear dynamic model of the crane and applied under three distinct cases involving different cable and payload lengths. Simulation results show that the multi-mode EI shaper (MM-EI) has the highest performance in reduction of the hook and payload oscillations, with the lowest maximum transient sway and mean average error. In addition, with 40% errors in the oscillation frequencies, the MM-EI provides the highest robustness by achieving 50% reductions in the payload oscillations as compared to the case with an unshaped input.

Keywords: Distributed mass payload; Double-pendulum; Input shaping; Multi-mode shaper; Overhead crane; Robust shaper.

1. INTRODUCTION

Cranes are type of machine that produce powerful strength commonly used in manufacturing, construction and transport sectors to convey bulky, dangerous and lift heavyweight load from one spot to another in between the workspace. There are different types of cranes which can be categorised depending on the mode of movement and structures: (a) Boom and tower cranes, and (b) Overhead and bridge cranes [1]. Overhead cranes are designed to lift, lower, and traverse horizontally along a rail or beam, possessing the capacity to safely handle extremely heavy loads [2]. Utilising an overhead crane is a more practical and efficient solution for transporting large or exceptionally heavy materials within a manufacturing facility, eliminating the challenges and difficulties associated with operating through congested pathways and limited floor space.

While there is a substantial body of research on the dynamics and control of cranes in the literature, most of these studies have concentrated on the Point-Mass Payload (PMP) scenario, with less attention devoted to other payload configurations like distributed mass payloads (DMP). Recent research has shifted its focus from the traditional PMP to the more realistic DMP's for double-pendulum cranes, reflecting a growing interest in more accurate and practical modelling [3]. The primary difference between PMP and DMP in a crane system is the way the payload's weight is treated and incorporated into the system's dynamics. The PMP model simplifies the payload's weight by concentrating it at a single point, making calculations easier, but potentially overlooking the complexity of real-world situations where the weight is distributed across the payload [4]. In contrast, the DMP model considers the actual distribution of weight within the payload, providing a more precise representation of its impact on the crane's performance and structural stability. However, the attachment of such a payload to the hook using multiple rigging cables results in complex crane dynamics. Furthermore, the crane dynamics behave as a double-pendulum crane and oscillates with multi-mode frequencies [5]. When in operation, the crane's hook and payload move in synchronized oscillations, requiring a control system that accounts for all oscillation modes to achieve precise and stable control [6]. Dynamic modelling and characterisation of an overhead crane carrying a DMP was presented in [4], together with the study on the influence of changing crane and DMP parameters on the system dynamics.

Control algorithms for an overhead crane with DMP can be divided into two main categories: closed-loop and open-loop techniques. As the closed-loop techniques can be used for position and oscillation control of the crane, they have received more attention from researchers. The proposed techniques include an adaptive control system for precise positioning and swing reduction of 3-D overhead cranes [7], a wave-based control that was not depended on the accuracy of the system model [8], time-varying Sliding Mode Control (SMC) [9], [10], equivalent rope length trajectory planning [11], adaptive fuzzy tracking control systems [12], time-optimal anti-swing control based on low-pass filter [13] and deep reinforcement learning-based control [14]. On the other hand, the open-loop techniques have the advantage of being simpler to implement and more cost-effective than the closed-loop methods. They were mainly used for control of crane oscillation. The proposed open-loop techniques for a DMP system include a command smoothing control combining low-pass and multi-notch filters [3], command smoothing control based on the modelled damped oscillation period [15], Extra-insensitive (EI) and modified EI shaper for control of dual cranes under a planar motion [16], discontinuous piecewise and hybrid piecewise smoothers [17], and an ANN-based optimal command smoother [18]. However, basic input shaping techniques lack robustness, particularly with uncertain parameters and external disturbances, making them less robust than the closed-loop approaches [19].

Review of existing research on double-pendulum overhead crane (DPOC) with DMP reveals that achieving effective control remains a difficult task, and currently, there is no single control strategy that can successfully minimise both hook and payload oscillations to an optimal level. As the crane is a multi-mode system and oscillates with two different frequencies, an effective open-loop technique that can handle both oscillations is desirable. This paper investigates design and performance analyses of multi-mode robust input shapers for oscillation control of an overhead crane carrying DMP. Three robust shapers which are based on EI, Zero Vibration Derivative (ZVD) and Equal Shaping-Time and Magnitudes (ETM) are designed and simulated utilising a nonlinear dynamic model of the system. The main contribution of this work lies in the design of multi-mode shapers applied to a crane carrying DMP. Three cases with distinct cable and payload lengths are examined to evaluate the control performance in terms of reductions of hook and payload oscillations. Robustness of the shapers is also examined by considering 40% error in the hook and payload oscillation frequencies.

2. DYNAMIC MODEL OF AN OVERHEAD CRANE

Modelling of a DPOC system with DMP was achieved through utilisation of the Lagrangian approach. Figure 1 depicts a schematic diagram of a DPOC carrying a DMP with a constant cable length. The crane has three independent generalised coordinates which are trolley position, hook and payload angles denoted by x, θ, and φ respectively. The only input for the system is an applied external force, F_x. Modelling of the crane carrying DMP using Lagrangian method was described in details in [4]. This work utilised the derived dynamic model for extensive simulation work.

The nonlinear dynamic model of the crane system can be written as [4]

$$\begin{gathered}\left(m_t + m_h + m_p\right)\ddot{x} - \left(m_h + m_p\right)l_1\ddot{\theta}\cos\theta + \left(m_h + m_p\right)l_1\dot{\theta}^2\sin\theta \\ -m_p l_2\ddot{\varphi}\cos\varphi + m_p l_2\dot{\varphi}^2\sin\varphi = F - f_x\dot{x}\end{gathered} \tag{1}$$

$$\begin{gathered}-\left(m_h - m_p\right){l_1}^2\ddot{\theta} - \left(m_h + m_p\right)l_1\ddot{x}\cos\theta \\ + m_p l_1 l_2\ddot{\varphi}\cos(\theta - \varphi) + m_p l_1 l_2\dot{\varphi}^2\sin(\theta - \varphi) + \left(m_h + m_p\right)g l_1\sin\theta = 0\end{gathered} \tag{2}$$

$$m_p\left({l_2}^2 + \frac{1}{12}{l_p}^2\right)\ddot{\varphi} - m_p l_2\ddot{x}\cos\varphi + m_p l_1 l_2\ddot{\theta}\cos(\theta - \varphi) - m_p l_1 l_2\dot{\theta}^2\sin(\theta - \varphi) + m_p g l_2\sin\varphi = 0 \tag{3}$$

Where all the symbols are as described in Table 1. Equations (1) – (3) show that the system is highly nonlinear, and all the outputs are coupled. Table 1 lists the crane parameters and their values used in this simulation work. These values were taken from a laboratory overhead crane as described in [4].

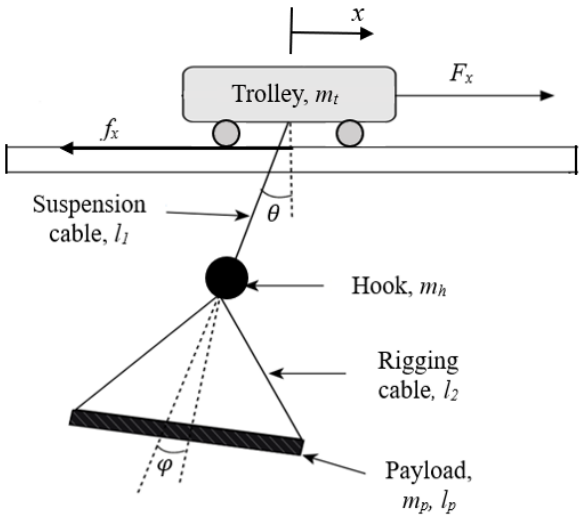

Figure 1. DPOC system with DMP.

Table 1. Overhead crane parameters.

Variables	Symbol	Values/units
Mass of trolley	m_t	1.155 kg
Mass of hook	m_h	0.1 kg
Mass of payload	m_p	0.215 kg
Cable length between trolley and hook	l_1	0.3, 0.4, 0.5 m
Cable length between hook and payload	l_2	0.2 m
Horizontal length of the DMP	l_p	0.2, 0.3, 0.4 m
Viscous damping coefficients of trolley	f_x	82 Ns/m
Gravitational constant	g	9.81 m/s^2

3. INPUT SHAPING TECHNIQUES

The basic concept of the input shaping technique is to obtain an input that is able to reduce system's vibration and oscillation. This technique has become popular among researchers as its implementation is easier and it is able to move an underactuated system without causing vibration. This is an open-loop technique in which the base command and the delay part of the base command are used to implement command shaping and cancel the vibration [20], [21]. The design objective is to determine amplitudes and time locations of impulses which can be obtained by using the system's natural frequency and damping ratio. In this work, three robust shapers are designed with different impulse magnitudes and locations. They are briefly described in the following sections.

3.1 Zero Vibration Derivative (ZVD) Shaper

For any vibratory system, the output y_0 can be expressed as:

$$y_0 = \left[\frac{A_0\omega}{\sqrt{1-\zeta^2}}e^{-\zeta\omega(t-t_0)}\right]\sin(\omega\sqrt{1-\zeta^2}(t-t_0)) \tag{4}$$

where A_0 is the amplitude of impulse applied, ζ is the damping ratio and ω is the natural frequency of the system. Zero Vibration (ZV) shaper is the simplest type of input shaping technique with two impulses, and the amplitudes and time locations of the impulses can be calculated as:

$$\begin{bmatrix}A_i\\t_i\end{bmatrix} = \begin{bmatrix}\frac{1}{1+K} & \frac{K}{1+K}\\0 & \frac{\pi}{\omega_d}\end{bmatrix} \tag{5}$$

where

$$\omega_d = \omega_n\sqrt{1-\zeta^2} \quad \text{and} \quad K = e^{-\frac{\pi\zeta}{\sqrt{1-\zeta^2}}} \tag{6}$$

However, the ZV shaper is not robust as small adjustments/errors in the damping ratio and natural frequency significantly degrade its performance. An additional constraint was later added into the formulation to improve the performance of the ZV shaper in the presence of nonlinearities, modelling errors, and parameter uncertainties [22]. This additional constraint causes the frequency derivative of residual vibration to become zero. Solving the related equations yields a three-impulses input shaper known as Zero Vibration Derivative (ZVD) shaper as shown in Figure 2. The magnitudes and locations of the shaper can be determined as:

$$\begin{bmatrix}A_i\\t_i\end{bmatrix} = \begin{bmatrix}A_1 & A_2 & A_3\\t_1 & t_2 & t_3\end{bmatrix} \tag{7}$$

where

$$A_1 = \frac{1}{(1+K)^2}, A_2 = \frac{2K}{(1+K)^2}, A_3 = \frac{K^2}{(1+K)^2}, t_1 = 0, t_2 = \frac{\pi}{\omega_d}, t_3 = \frac{2\pi}{\omega_d}$$

3.2 Extra-Insensitive (EI) Shaper

The ZVD shaper is designed with an extended shaper duration and a more gradual response to enhance the robustness of ZV shapers. In order to solve this problem, an alternative shaper was designed by adding a constraint to reduce vibration [23]. This shaper offers an additional resistance to errors in the natural frequency and damping ratio estimation. The shaper is known as Extra-Insensitive (EI) shaper which has a comparable duration to that of the ZVD shaper but with greater robustness. The development of the EI shaper involves the use of three impulses having the same locations as the ZVD shaper, however with varying amplitudes. The amplitude and time location of impulses for the EI shaper can be obtained as [24]

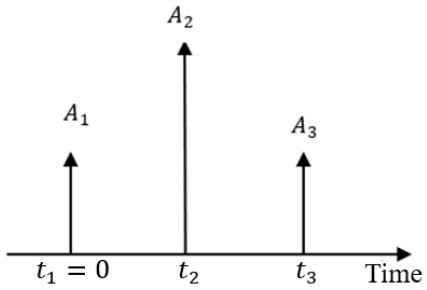

Figure 2. ZVD shaper with three impulses.

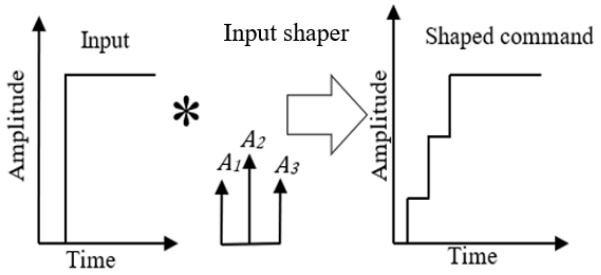

Figure 3. Input shaping process.

$$\begin{bmatrix} A_i \\ t_i \end{bmatrix} = \begin{bmatrix} \frac{1+V_{tol}}{4} & \frac{1-V_{tol}}{2} & \frac{1+V_{tol}}{4} \\ t_1 & t_2 & t_3 \end{bmatrix} \tag{8}$$

where V_{tol} is defined as the acceptable level of vibration, typically set at 5% or 0.05. t_1, t_2 and t_3 are similar to the ZVD shaper as in Equation (7).

3.3 Equal Shaping-Time and Magnitudes (ETM) Shaper

The concept of Equal Shaping-Time and Magnitudes (ETM) shapers is based on impulse vectors and input shaping as described in [25]. The ETM shaper is a specific type of shaping technique that involves shaping impulses with equal magnitudes and time locations. In this technique, impulses with the same magnitude and the same angle between impulse vectors are applied, contributing to the optimisation of the system's response and reducing undesired vibrations [25], [26].

The ETM shaper ensures that the sum of its impulse vectors is consistently zero for all $n \geq 2$ (n is the number of impulse), distinguishing it from the ZVD or EI shapers [27]. Notably, the shaping time remains fixed at one damped period of the time response, irrespective of the increase in n. Derived from these conditions, the ETM4 shaper, featuring four impulse vectors, can be obtained as:

$$\begin{bmatrix} A_i \\ t_i \end{bmatrix} = \begin{bmatrix} \frac{I}{1+m} & \frac{I}{\tau^{\frac{2}{3}}} & \frac{I}{\tau^{\frac{4}{3}}} & \frac{mI}{(1+m)\tau^2} \\ 0 & \frac{(2\pi/3)}{\omega_d} & \frac{(4\pi/3)}{\omega_d} & \frac{2\pi}{\omega_d} \end{bmatrix} \tag{9}$$

where

$$I = \frac{(1+m)\tau^2}{\tau^2 + (1+m)(\tau^{\frac{4}{3}} + \tau^{\frac{2}{3}}) + m}, \quad \tau = e^{\zeta\pi/\sqrt{1-\zeta^2}} \tag{10}$$

and $m = 0.79$ and 0.9 for the hook and the payload shaper designs respectively. It is worth mentioning that ETM3 shaper with the parameter m set to 1 is similar to the ZVD shaper.

3.4 Design of Multi-Mode Shapers

Generally, the shaping process is as shown in Figure 3 where a desired input is convolved with an input shaper to yield a shaped command. The shaped command is then excited into the system for reduction of oscillation. However, as the overhead crane with DMP oscillates with two modes of frequencies for the hook and payload, it is necessary to design an input shaper that considers all the frequencies. In this case, reduction of hook oscillation is crucial in order to achieve low payload oscillation as both hook and payload responses are highly coupled. In this work, design of a multi-mode shaper is proposed, in which two different shapers are designed separately based on the two frequencies and damping ratios. Then, both shapers are convolved to obtain a single multi-mode shaper. Figure 4 shows a block diagram of designing the multi-mode shaper and its implementation for oscillation control in an open-loop configuration.

In this work, multi-mode EI (MM-EI), ETM4 (MM-ETM4), and ZVD (MM-ZVD) shapers were designed and simulated for control of the crane. Each technique provided different shaper parameters as in Equations (7) – (9), and comparative assessments of their performance and robustness can be conducted.

4. IMPLEMENTATION AND RESULTS

This section presents design and implementation of the multi-mode shapers, and simulation results of the crane oscillation responses. The controller's performance and robustness are examined and discussed.

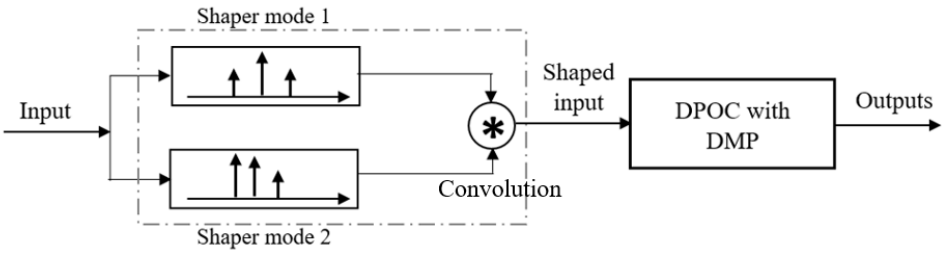

Figure 4. Design and implementation of multi-mode input shapers.

4.1 Implementation

Three cases of crane parameters with distinct cable and payload lengths were considered to evaluate the controller's performance and robustness. The cases are:

a) Case 1: cable length of 0.30 m and DMP length of 0.20 m.
b) Case 2: cable length of 0.40 m and DMP length of 0.30 m.
c) Case 3: cable length of 0.50 m and DMP length of 0.40 m.

The other parameters are kept constant: hook mass (100 g), payload mass (215 g), and rigging cable length (0.2 m).

In order to design the multi-mode shapers, the oscillation frequency of the crane system need to be measured or estimated. For this purpose, the crane was initially excited with a trapezoidal input signal with an amplitude of 1 N and a time duration of 2 s as shown in Figure 5. The input was applied to the crane as an external force to move the trolley. This is a typical input given by an operator in which it is initially accelerated, then maintain at a maximum speed, and eventually decelerated to stop the crane.

Simulation of the nonlinear DPOC with DMP dynamic model given in Equations (1) – (3) and implementation of the controllers were performed using Matlab and Simulink R2021a version. A computer with i5 and 2.40 GHz processor, 12 GB RAM and 64-bit operating system was used. The simulation employed the ode45 (Dormand-Prince) solver with a variable step. For evaluation of the controller performance, the hook and payload oscillation responses were monitored for a duration of 10 s. Maximum transient sway (MTS) and mean average error (MAE) values were calculated and used as performance indexes of the controllers. MTS determines the maximum amplitude during the transient response whereas the MAE values indicate the average magnitude of the oscillations throughout the observation period. Lower MTS and MAE values are desirable as they represent low oscillation in the transient and overall responses.

4.2 Unshaped Input

Simulation results of the hook and payload oscillation responses when excited with the input shown in Figure 5 under the three cases are shown in Figure 6. It is noted that changes in the cable and payload lengths of the crane significantly impact the oscillatory behavior, influencing the amplitude, shape, and frequency of the oscillations. During these operations, the MTS for the hook decreases in a sequential order for each case, whereas the MTS for the payload oscillation increases.

Table 2 presents the oscillation frequencies of the hook and payload responses for all cases, revealing that the crane oscillates at different frequencies in each case. From Case 1 to Case 3, the hook and payload oscillation frequencies have reduced by 39%. These findings correspond with theoretical expectations, as increasing the cable length during operation leads to a decrease in the oscillation frequency. Furthermore, the results demonstrate that the DPOC with DMP exhibits a multi-mode behavior, characterised by multiple oscillation frequencies.

4.3 Shaped Input Responses

Based on the oscillation frequencies of the hook and payload oscillations of each case as shown in Table 2, magnitudes and time locations of EI, ETM4 and ZVD shapers were calculated separately. As an example, the calculated parameters of the shapers for Case 2 are presented in Table 3. The shapers for the hook and payload are then convolved to yield a multi-mode shaper as shown in Figure 4. Figure 7 shows the shaped inputs obtained after the original input (Figure 5) was modified using the multi-mode shapers.

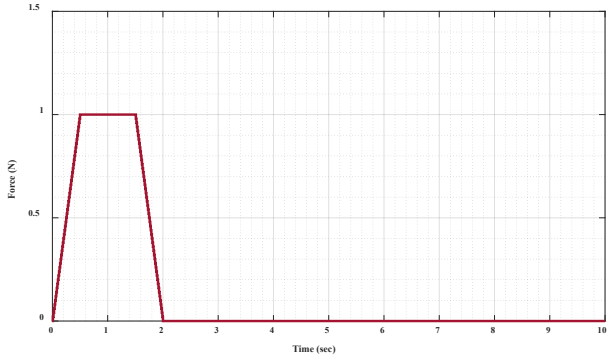

Figure 5. Input force signal.

Table 2. Hook and payload oscillation frequencies.

Modes	Case 1	Case 2	Case 3
Hook	5.05	5.01	3.09
Payload	5.43	5.28	3.30

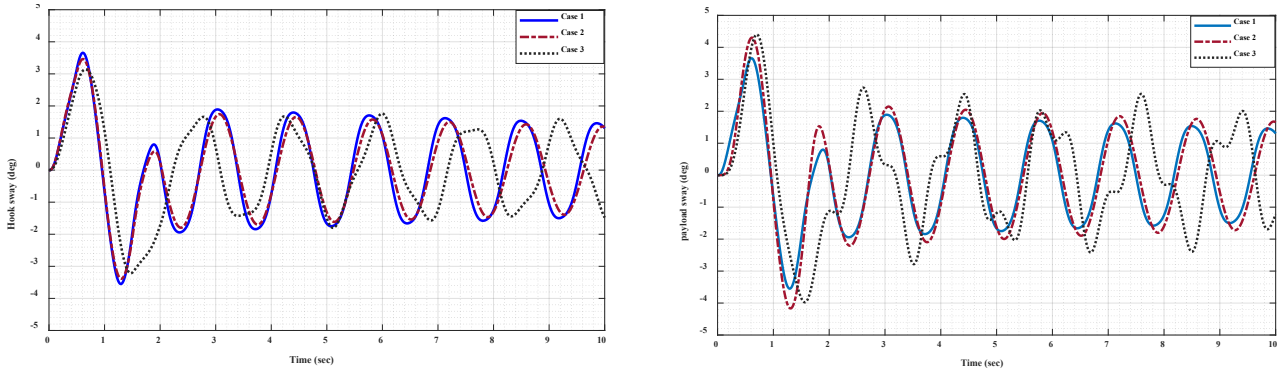

(a) (b)

Figure 6. Unshaped response of the DPOC system (a) Hook oscillation and (b) Payload oscillation.

Table 3. Shaper parameters for Case 2.

	Mode	Magnitudes				Time locations		
		A_1	A_2	A_3	A_4	t_2	t_3	t_4
Hook	ZVD	0.45	0.45	0.12	-	0.65	1.29	-
	ETM4	0.34	0.37	0.23	0.06	0.43	0.86	1.29
	EI	0.45	0.38	0.12	-	0.67	1.29	-
Payload	ZVD	0.36	0.48	0.16	-	0.6	1.20	-
	ETM4	0.26	0.36	0.28	0.10	0.40	0.80	1.20
	EI	0.38	0.44	0.18	-	0.6	1.20	-

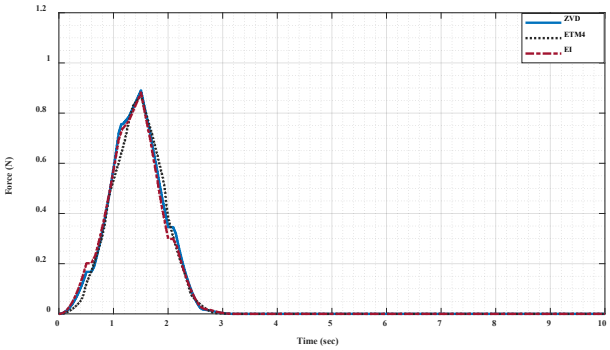

Figure 7. Shaped input signals

Figure 8 shows the hook and payload oscillation responses for Case 1 with the shaped inputs. It is noted that all the shaped inputs significantly reduced the oscillations as compared to the unshaped responses. MM-EI can also be shown to be superior as it produced the lowest MTS value and has the lowest overall oscillation. Figures 9 and 10 depict the oscillation response simulations for Cases 2 and 3 respectively, with the same input force as in Figure 5. Similarly, the results show that all the controllers significantly improved the system's performance. Moreover, a similar pattern was obtained in which the MM-EI outperformed the MM-ZVD and MM-ETM4 by achieving more substantial reductions. Figures 11 and 12 present comparative assessments of the shapers in terms of the MTS and MAE values. The results indicate that for all cases, the MM-EI provided the best performance in oscillation reductions with the lowest MTS and MAE values. This is further evidenced in Figure 13 with the percentage of improvements achieved by using all the shapers. As expected, the MM-ETM4 provided a better performance than the MM-ZVD shaper.

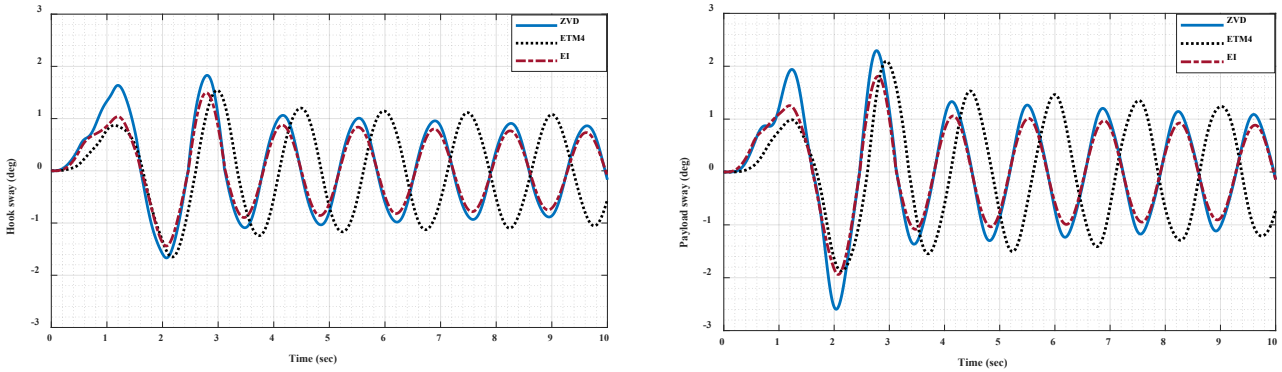

(a) (b)

Figure 8. Response of the DPOC for Case 1: (a) Hook oscillation and (b) Payload oscillation.

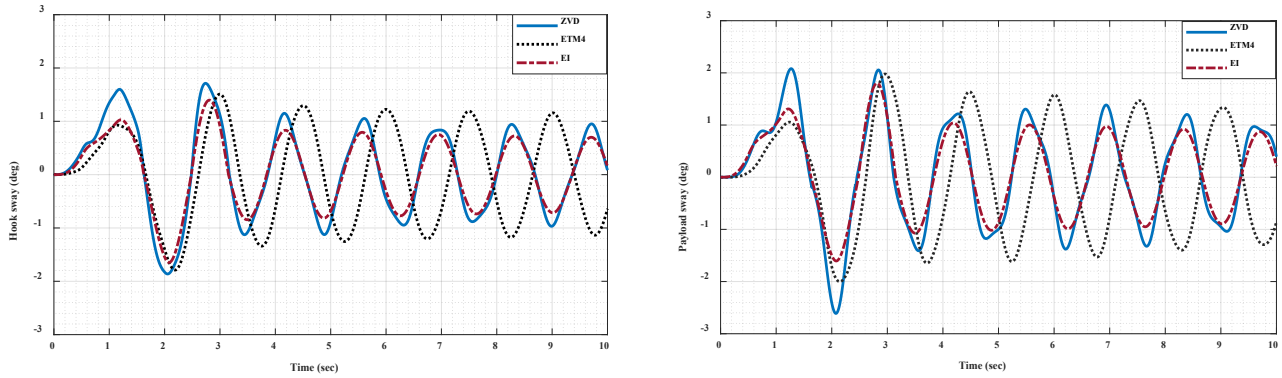

(a) (b)

Figure 9. Response of the DPOC for Case 2: (a) Hook oscillation and (b) Payload oscillation.

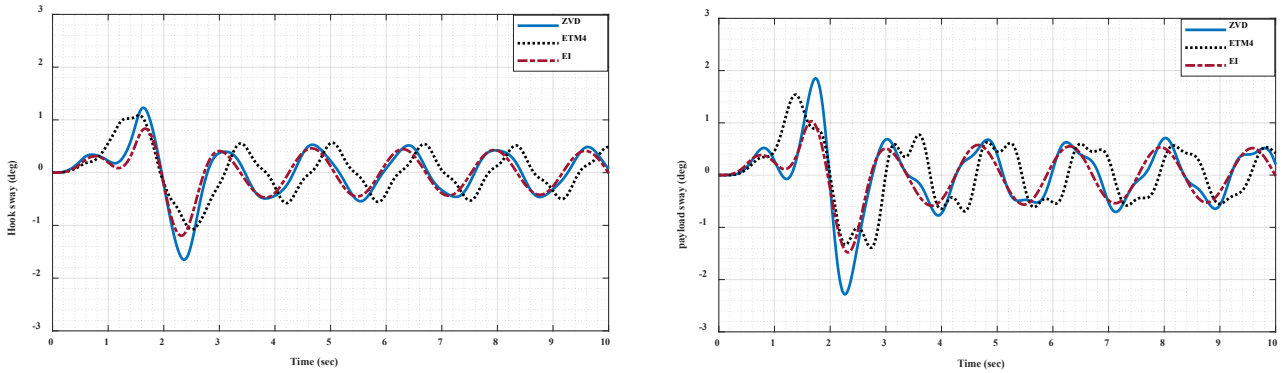

(a) (b)

Figure 10. Response of the DPOC for Case 3: (a) Hook oscillation and (b) Payload oscillation.

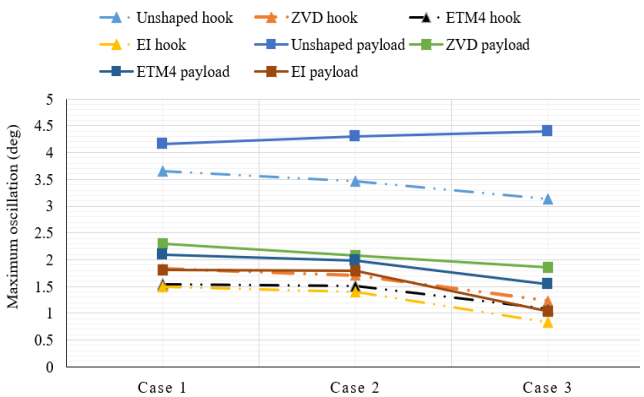

Figure 11. MTS of the crane oscillations with input shaper.

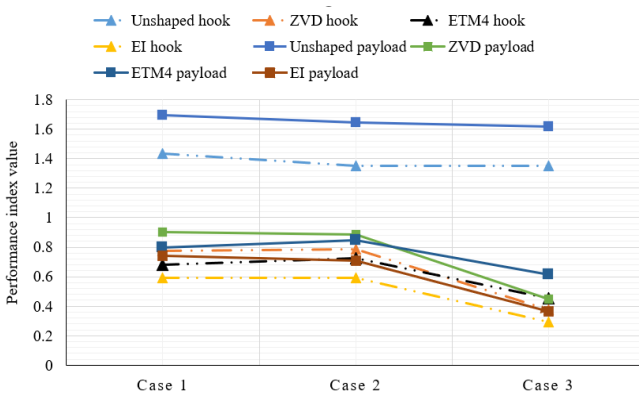

Figure 12. MAE of the crane oscillations with input shaper.

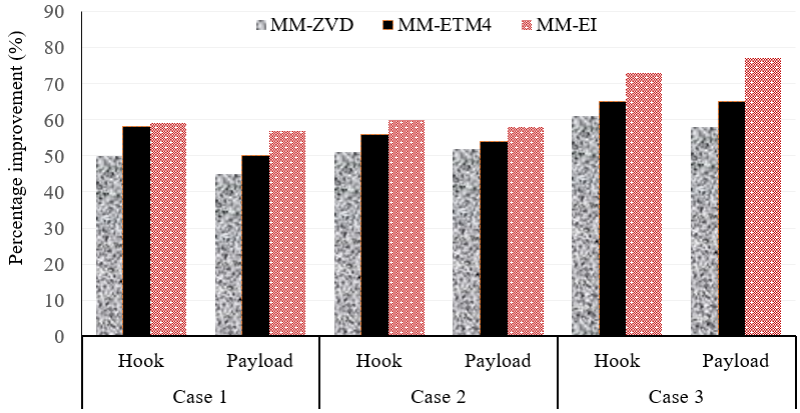

Figure 13. Percentage improvements as compared to the unshaped input.

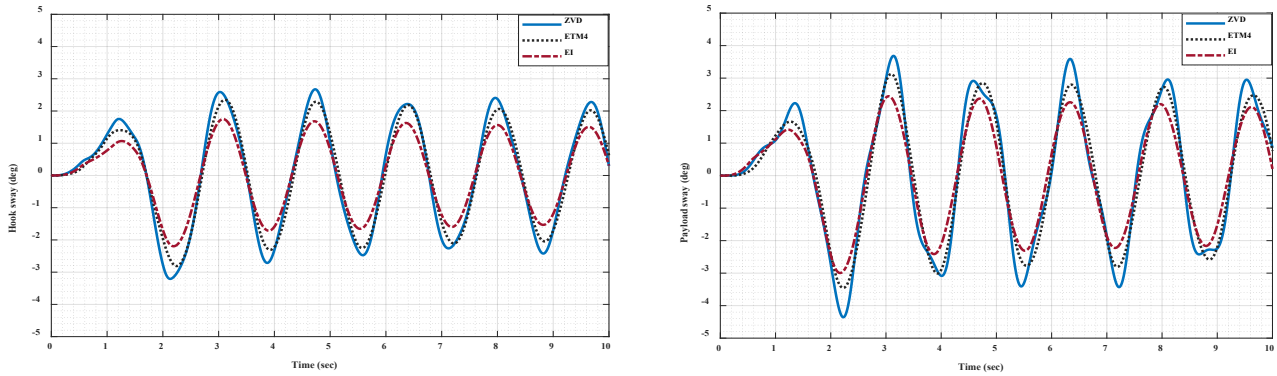

(a) (b)

Figure 14. Simulation responses with 40% errors in oscillation frequencies: (a) Hook oscillation and (b) Payload oscillation.

Table 4. Percentage of improvements with erroneous oscillation frequencies.

	MTS				MAE			
	Hook		Payload		Hook		Payload	
	Value (deg)	Improve (%)	Value (deg)	Improve (%)	Value (deg)	Improve (%)	Value (deg)	Improve (%)
Unshaped	3.46	-	4.30	-	1.35	-	1.64	-
MM-ZVD	2.67	22.8	3.61	16.1	1.34	0.74	1.60	2.44
MM-ETM4	2.35	32.1	3.03	29.5	1.19	11.9	1.41	14.0
MM-EI	1.75	49.4	2.16	49.7	0.90	33.3	1.12	31.7

4.4 Robustness Analysis

A major drawback of input shaping technique is its low robustness towards parameter uncertainties and measurement/estimation errors of crane parameters and oscillation frequencies. In this work, the robustness of all the robust shapers were examined by considering erroneous oscillation frequencies in the shaper designs. In this case, the multi-mode shapers with parameters designed using Case 2 shown in Table 2 were implemented for Case 3. This represents 40% errors in the hook and payload oscillation frequencies. Figure 14 shows the simulation responses of the oscillations using the multi-mode shapers with erroneous frequencies. As expected, the performance of all the shapers in reducing the oscillations decreased as compared to Figure 10 (Case 3 with exact frequencies). However, reasonable oscillation reductions were obtained using the MM-EI shaper.

Table 4 summarises the MTS and MAE values obtained using the shapers and their percentage of improvements as compared to the unshaped input. It can be shown that the MM-EI provided the highest robustness with 50% and 30% reductions in the MTS and MAE values. The MM-ETM4 only achieved 30% and 14% reductions in the oscillation responses.

5. CONCLUSION

Robust multi-mode shapers based on ZVD, EI and ETM4 input shapers have been designed for oscillation control of an overhead crane carrying DMP. Based on the system dynamics, separate input shapers considering the hook and payload oscillations were initially designed. Then, a multi-mode shaper was obtained by using a convolution process of both shapers. Matlab simulations utilising the nonlinear model of the crane under three cases involving different cable and payload lengths demonstrated that all the multi-mode shapers were able to provide significant hook and payload oscillations. Further analyses have shown the superiority of the MM-EI in reductions of oscillations with the lowest values of MTS and MAE. Furthermore, analyses with 40% error in the oscillation frequencies have also revealed that the MM-EI shaper has the highest robustness when compared to the other shapers.

ACKNOWLEDGEMENT AND FUNDING

The authors receive no financial support for the research, authorship, and publication of this article.

DECLARATION OF CONFLICTING INTERESTS

The authors declare no potential conflicts of interest with respect to the research and publication of this article.

REFERENCES

[1] L. Ramli, Z. Mohamed, A. M. Abdullahi, H. I. Jaafar and I. M. Lazim, Control strategies for crane systems: A comprehensive review, *Mechanical Systems and Signal Processing*, 95, 2017, 1-23.

[2] W. Singhose, Command shaping for flexible systems: A review of the first 50 years, *International Journal of Precision Engineering and Manufacturing*, 10(4), 2009, 153-168.

[3] J. Huang, Z. Liang and Q. Zang, Dynamics and swing control of double-pendulum bridge cranes with distributed-mass beams, *Mechanical Systems and Signal Processing*, 54-55, 2015, 357-366.

[4] M. M. Bello, Z. Mohamed, M. Ö. Efe and H. Ishak, Modelling and dynamic characterisation of a double-pendulum overhead crane carrying a distributed-mass payload, *Simulation Modelling Practice and Theory*, 134, 2024, 102953.

[5] H. I. Jaafar, Z. Mohamed, M. A. Shamsudin, N. A. Mohd Subha, L. Ramli and A. M. Abdullahi, Model reference command shaping for vibration control of multimode flexible systems with application to a double-pendulum overhead crane, *Mechanical Systems and Signal Processing*, 115, 2019, 677-695.

[6] H. I. Jaafar, Z. Mohamed, M. A. Ahmad, N. A. Wahab, L. Ramli and M. H. Shaheed, Control of an underactuated double-pendulum overhead crane using improved model reference command shaping: Design, simulation and experiment, *Mechanical Systems and Signal Processing*, 151, 2021, 107358.

[7] L. Yang and H. Ouyang, Precision-positioning adaptive controller for swing elimination in three-dimensional overhead cranes with distributed mass beams, *ISA Transactions*, 127, 2022, 449-460.

[8] W. O'Connor and H. Habibi, Gantry crane control of a double-pendulum, distributed-mass load, using mechanical wave concepts, *Mechanical Sciences*, 4(2), 2013, pp. 251-261.

[9] T. Wang *et al.*, A time-varying sliding mode control method for distributed-mass double pendulum bridge crane with variable parameters, *IEEE Access*, 9, 2021, 75981-75992.

[10] Q. Wu, X. Wang, L. Hua and M. Xia, Modeling and nonlinear sliding mode controls of double pendulum cranes considering distributed mass beams, varying roped length and external disturbances, *Mechanical Systems and Signal Processing*, 158, 2021, 107756.

[11] Q. Wu, N. Sun and X. Wang, Equivalent rope length-based trajectory planning for double pendulum bridge cranes with distributed mass payloads, *Actuators*, 11(1), 2022, 25.

[12] Z. Sun and H. Ouyang, Adaptive fuzzy tracking control for vibration suppression of tower crane with distributed payload mass, *Automation in Construction*, 142, 2022, 104521.

[13] Q. Wu, X. Wang, L. Hua and M. Xia, Improved time optimal anti-swing control system based on low-pass filter for double pendulum crane system with distributed mass beam, *Mechanical Systems and Signal Processing*, 151, 2021, 107444.

[14] Q. Wu, N. Sun, T. Yang and Y. Fang, Deep reinforcement learning-based control for asynchronous motor-actuated triple pendulum crane systems with distributed mass payloads, *IEEE Transactions on Industrial Electronics*, 71(2), 2024, 1853-1862.

[15] J. Huang, X. Xie, and Z. Liang, Control of bridge cranes with distributed-mass payload dynamics, *IEEE/ASME Transactions on Mechatronics*, 20(1), 2015, 481–486.

[16] X. Zhao and J. Huang, Distributed-mass payload dynamics and control of dual cranes undergoing planar motions, *Mechanical Systems and Signal Processing*, 126, 2019, 636-648.

[17] J. Ye and J. Huang, Control of beam-pendulum dynamics in a tower crane with a slender jib transporting a distributed-mass load, *IEEE Transactions on Industrial Electronics*, 70(1), 2023, 888-897.

[18] X. Miao, L. Yang and H. Ouyang, Artificial-neural-network-based optimal Smoother design for oscillation suppression control of underactuated overhead cranes with distributed mass beams, *Mechanical Systems and Signal Processing*, 200, 2023, 110497.

[19] A. M. Abdullahi, M. F. Hamza, Z. Mohammed, M. M. Bello, M. Attahir and F. A. Darma, Distributed delay adaptive output-based command shaping for different cable lengths of double-pendulum overhead cranes, *International Journal of Dynamics and Control,* 12, 2024, 1466-1476.

[20] S. Fasih, Z. Mohamed, A. Husain, L. Ramli, A. Abdullahi and W. Anjum, Payload swing control of a tower crane using a neural network-based input shaper, *Measurement and Control*, 53(7-8), 2020, 1171-1182.
[21] S. M. F. ur Rehman, Z. Mohamed, A. R. Husain, L. Ramli, A. M. Abbasi, W. Anjum and M. H. Shaheed, Adaptive input shaper for payload swing control of a 5-DOF tower crane with parameter uncertainties and obstacle avoidance, *Automation in Construction*, 154, 2023, 104963.
[22] A. M. Abdullahi, Z. Mohamed, H. Selamat, H. R. Pota, M. S. Zainal Abidin and S. M. Fasih, Efficient control of a 3D overhead crane with simultaneous payload hoisting and wind disturbance: design, simulation and experiment, *Mechanical Systems and Signal Processing*, 145, 2020, 106893.
[23] W. Singhose, S. Derezinski and N. Singer, Extra-insensitive input shapers for controlling flexible spacecraft, *Journal of Guidance, Control, and Dynamics*, 19(2), 1996, 385-391.
[24] J. Cao, M. Yang, Q. Ni and D. Xu, An improved extra-insensitive input shaper with feed-forward compensation for servo systems, *IEEE International Conference on Electrical Systems for Aircraft, Railway, Ship Propulsion and Road Vehicles & International Transportation Electrification Conference (ESARS-ITEC)*, Nottingham, UK, 2018, 1-5.
[25] C. -G. Kang, Impulse vectors for input-shaping control: A mathematical tool to design and analyze input shapers, *IEEE Control Systems Magazine*, 39(4), 2019, 40-55.
[26] C. -G. Kang and S. -G. Lee, Impulse vector: A basic mathematical tool to design and analyze flexible robots for removing residual vibrations, *20th International Conference on Ubiquitous Robots (UR)*, Honolulu, USA, 2023, 6-12.
[27] W. Singhose, W. Seering and N. Singer, Residual Vibration Reduction Using Vector Diagrams to Generate Shaped Inputs, *Journal of Mechanical Design*, 116(2), 1994, 654-659.